Available online at www.sciencedirect.com

ScienceDirect

journal homepage: www.elsevier.com/locate/he

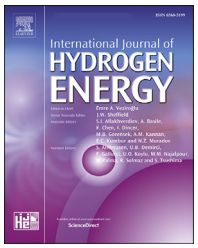

Trash to treasure: A novel chemical route to synthesis of NiO/C for hydrogen production

Shun Lu [a], Matthew Hummel [a], Zhengrong Gu [a,*], Yan Gu [a], Zhisheng Cen [a], Lin Wei [a], Yue Zhou [b], Caizhi Zhang [c], Chi Yang [d,**]

[a] Department of Agricultural and Biosystems Engineering, South Dakota State University, Brookings, SD 57007, USA
[b] Department of Electrical Engineering and Computer Science, South Dakota State University, Brookings, SD 57007, USA
[c] School of Automotive Engineering, The State Key Laboratory of Mechanical Transmissions, Chongqing, Automotive Collaborative Innovation Center, Chongqing University, Chongqing 400044, China
[d] Yale-NUIST Center on Atmospheric Environment, Nanjing University of Information Science and Technology, Jiangsu 210044, China

ARTICLE INFO

Article history:
Received 8 February 2019
Received in revised form
14 April 2019
Accepted 18 April 2019
Available online 14 May 2019

Keywords:
Eggshell membrane
NiO
Electrocatalyst
Hydrogen evolution reaction

ABSTRACT

Transition metal oxides (TMOs), especially nickel oxide (NiO), are environmentally benign and cost-effective materials, and have recently emerged as potential hydrogen evolution reaction (HER) electrocatalysts for future industrial scale water splitting in alkaline environment. However, their applications in HER electrocatalysts remain challenging because of poor electronic conductivity and unsatisfactory activity. Besides, the disposal of eggshell waste is also an environmentally and economically challenging problem as a result of food industry. Here, we report the synthesis of NiO nanoparticles (NPs) encapsulated in the carbonization of eggshell membrane via a green and facile approach for HER application. Noteworthy to mention here that the active carbon was made from the waste, eggshell membrane (ESM), meanwhile, the eggshell was used as a micro-reactor for preparation of electrocatalyst, NiO/C nanocomposite. Then, the as-prepared NiO/C nanocomposite was characterized by scanning electron microscopy (SEM), transmission electron microscopy (TEM), X-ray diffraction (XRD) and energy dispersive x-ray spectroscopy (EDS). The SEM, EDS and TEM images reveal that NiO nanoparticles distributed on the carbon support, and XRD patterns confirm the presence of the nanoparticles are NiO and C hybrids. The catalytic activity and durability of NiO/C nanocomposite was examined for HER in 1 M KOH solution. It has been observed that NiO/C nanocomposite showed the better catalytic activity with the smallest Tafel slope of 77.8 mV dec^{-1} than single component's result, NiO particles (112.6 mV dec^{-1}) and carbonization of ESM (94.4 mV dec^{-1}). It indicates that the HER performance of electrocatalyst can be enhanced by synergistic effect between NiO particles and carbonization of ESM, with better durability after 500 CV cycles. Furthermore, such design principle for developing interfaces between TMOs and C by a green and facile method can offer a new approach for preparing more efficient electrocatalysts.

* Corresponding author.
** Corresponding author.
E-mail addresses: Zhengrong.Gu@sdstate.edu (Z. Gu), yangchi@seu.edu.cn (C. Yang).
https://doi.org/10.1016/j.ijhydene.2019.04.191

Introduction

Hydrogen (H_2) with high gravimetric energy density and environmental friendliness, has made H_2 as an ideal energy carrier alternative to the diminishing fossil fuels [1–3]. Hydrogen evolution reaction (HER) from electrolysis of alkaline water is generally regarded as a more promising approach due to alkaline water splitting is more practical for industry than the traditional steam-reforming route ($CH_4 + H_2O \rightarrow H_2 + CO$), which suffers from expensive cost and low purity [4,5]. Generally, multiple elemental reactions result in the accumulation of energy barriers and further decrease the electrochemical kinetic of the key half reaction of HER during alkaline water splitting. In addition, HER process in alkaline, the so-called Volmer step, the water dissociation, is identified as the rate-determining step (RDS). However, its sluggish reaction kinetics and hinders the overall HER process. To date, Pt-based materials are still the benchmark electrocatalysts for HER both in acidic and alkaline medium [6–8]. However, their scarcity and high cost are major drawbacks in their large-scale commercialization. Therefore, it is mandatory to develop a cost-effective, non-noble HER electrocatalyst in alkaline environment with better performance [9,10].

In recent years, transition metal oxides (TMOs), especially nickel oxide (NiO), have shown high electrocatalytic activity towards HER application [4,10]. NiO, an important p-type semi-conductive transition metal oxide, has attracted widespread interest as electrode material in various applications [11], such as supercapacitors [12], Li-ion batteries [13] and fuel cell electrodes [14], due to its high theoretical capacity (2584 F g^{-1}) and cost-effectiveness [12]. Just like most of the transition metal oxides, they could be also used as HER electrocatalysts [15]. However, the application of NiO as HER catalyst has been hindered due to its large onset potential, which in turn results from its internal weakness, (I) electric conductivity and (II) accessible surface area. Many efforts have been tried to solve these issues, for instance, Yu et al. [12]prepared hierarchical flower-like NiO/NCHS composite (NCHS means N-doped carbon hollow spheres) for supercapacitor. This strategy not only provides conductive matrix with fast electron/ion transportation, but also increases more electrochemical active surface area for the as-prepared supercapacitor. Chinnappan et al. [16]fabricated C@NiO/Ni nanofibers via a simple electrospinning approach and examined their HER performance. Yang et al. [17]prepared NiO/C nanofibers composites derived from metal-organic framework compound as electrode materials for supercapacitors. We can easily found that metal foam and carbon materials are often used as common conductive matrixes, which could improve the conductivity as well as increase the structural stability in electrochemical fields [10,12]. Synergistic effect also is an important strategy to improve HER performance of composites. For example, Yu et al. [18]reported that Ni/NiO nanohybrids anchored on $CoSe_2$ nanobelts or carbon nanotube (CNT) sidewalls have shown superior HER performances as a result of the synergistic effect between metallic nickel and NiO. According to the above examples, it has been observed that NiO has an excellent performance as an electrocatalyst and is considered one of the most promising candidates in several experimental conditions.

The disposal of eggshell waste also attracted much attention due to its environmental and economical challenging problems [19–22]. 'Trash to Treasure' also becomes an interesting and important topic for those wastes, especially for eggshell and eggshell membrane (ESM) [19,23,24]. Deng et al. [19]demonstrated a novel application of waste eggshell as a multifunctional reaction system for the preparation of Co_9S_8 nanorod arrays on carbon fibers and put forward a new strategy of making use of eggshell to achieve *in situ* carbonization and sulfurization. Besides, numerous NiO/ESM-based materials with novel structures have been investigated and reported in the literature, such as NiO-Ni nanowires on carbonized eggshell membrane (Li-ion batteries) [25], porous C@$CoFe_2O_4$ nanocomposites derived from eggshell membrane (microwave absorption) [26], and SnO_2@ESM(energy storage) [27]. It has been observed that eggshell membrane plays vital important roles in energy storage and conversion according to the above examples [28,29]. Additionally, it is important to find that more active sites are easily found to absorb, activate and convert reactants at the interfaces [30]. However, few HER investigations of NiO/C composite derived from $Ni(OH)_2$/ESM have been reported in the literature.

In the present work, eggshell membrane was selected as the carbon source for the construction of NiO/C nanocomposite to achieve integrated use of eggshell waste as a micro-reactor, and eggshell membrane as functional biotemplate. This kind of structure not only enhances the conductivity of composites, but also can provide robust support for functional group. Herein, NiO/C nanocomposites were prepared via a facile and green approach. $Ni(OH)_2$/ESM was obtained through self-assembly of $Ni(OH)_2$ grown on the ESM surface in an alkaline solution ($urea + H_2O \rightarrow CO_2 + 2NH_3$). By subsequent, the NiO/C nanocomposite was successfully constructed with large surface area after carbonization under N_2 atmosphere. To our best of our knowledge, there is no article on the electrocatalyst for HER application of NiO/C nanocomposites prepared using eggshell membrane. The as-prepared NiO/C nanocomposite as HER electrocatalyst exhibited better performance than pure NiO particles and carbonization of ESM. The novel design outlined in this paper provides new utility for eggshell waste while also creating *in situ* functional nanocomposites.

Experimental

Materials

Nickel (II) nitrate hexahydrate [$Ni(NO_3)_2$ $6H_2O$] and urea (CH_4N_2O) were purchased from ACROS organics™. Nafion (5%) was obtained from Alfa Aesar Co., Ltd. Commercial activated carbon was gotten from Fisher Scientific Co., Ltd. Eggshell waste both eggshell and eggshell membrane (ESM) was obtained from fresh hen eggs purchased from Walmart by removing the liquid content of yolk and white via a hole cut in the eggshell. The eggshell waste with its membrane was washed by deionized water (DIW). DIW (>18.4 MΩ cm^{-1}) was used for preparation of aqueous solution, and all the

chemicals used in this investigation were analytical grade and were used without further purification.

Preparation of the NiO/C nanocomposites

In a typical procedure, NiO/C nanocomposites were obtained using a two-step method with minor revision [31,32]. To the eggshell "container", a 25 mL water solution of 0.4 M $Ni(NO_3)_2$ $6H_2O$ was added (inside), then the eggshell reactor was partially immersed in a 40 mL solution with 0.4 M urea inside a beaker, and the two solutions were separated by an eggshell with its membrane. The reactor was transferred into oven and maintained at 70 °C for 6 h. The as-coated eggshell membrane pieces were peel off from eggshell and washed with water thoroughly and dried in a vacuum oven (60 °C for 4 h). The color changed from the white bare ESM to a light green when coated with $Ni(OH)_2$. Secondly, the as-coated ESM was then heated at a ramp rate of 15 °C/min to 300 °C and kept at the set temperature for 1 h under N_2 protection, then continued heated at a ramp rate of 10 °C/min to 500 °C. Finally, the product (NiO/C) was then cooled to room temperature with N_2 protection. Aside from, the compared samples, NiO powders and carbonization of ESM, were prepared with same procedures, respectively.

Fabrication of working electrodes

Initially, a glassy carbon electrode (GCE) was polished to remove any form of contaminants from the surface. The as-prepared catalyst (4 mg) was dispersed in water/ethanol solution with a volume ratio of 1:1 (with the total volume of 2 mL). The mixture was kept under continuous sonication at (frequency of sonicator) for (time of sonication) to obtain a homogenous catalyst ink. 6 μL of this ink (2 mg/mL) was coated onto the surface of a polished GCE with a diameter of 4 mm, then 6 μL nation solution was dropped on the modified GCE in order to keep the catalyst ink stable and enhance its conductivity. It was dried under ambient environment to obtain a uniform catalyst film with geometric surface area of 0.1256 cm^2 and the mass loading of active materials was about ~0.09 mg/cm^2. The modified electrodes containing NiO/C nanocomposites, NiO powders, carbonization of ESM were named as NiO/C@GCE, NiO/GCE and C/GCE respectively.

Characterization

The crystalline information and morphology of those samples were characterized by X-ray diffraction (XRD) with Cu Kα irradiation (λ = 1.54056 Å), Scanning electron microscopy (SEM, FEI Siri200), Transmission electron microscopy (TEM, JEOL 2100F) under an acceleration voltage of 200 kV and element mapping on a Philips Tecnai G2 microscope. All the electrochemical tests were performed on an electrochemical workstation (BioLogic SP-150, France). The electrochemical impedance (EIS) study was performed within frequency range of 100 kHz to 0.1 Hz with an AC amplitude of 10 mV.

Electrochemical measurements

All the electrochemical measurements were performed on a BioLogic potentiostat/galvanostat/EIS analyzer (SP-150, France) in a typical three-electrode system consisting of the working electrode (WE), counter electrode (CE) and reference electrode (RE). Herein, the glassy carbon electrode (GCE, Φ = 4 mm) coated with the as-prepared catalyst loading was used as the WE, the Pt wire and the saturated Ag/AgCl electrode as the CE and RE, respectively. The mass loading of active materials was about 0.03 mg/cm^2. The HER performance was investigated by cyclic voltammetry (CV) and linear sweep voltammetry (LSV) which conducted from −0.8 to −1.8 V with a scan rate of 5 mV/s in 1 M KOH. EIS measurements were performed inside the three-electrode electrochemical cell. The Nyquist plot was carried out with overpotential of 135 mV and over a frequency range of 0.1–10^6 Hz. An equivalent Randles circuit model was used to fit the data to calculate the charge transfer resistance R_{ct} for each catalyst system. All potentials were referenced to the reversible hydrogen electrode (RHE) scale according to the Nernst equation. ($E_{RHE} = E_{Ag/AgCl} + 0.059^{*}pH + 0.21$ V, 25 °C). The collected data were IR-corrected for an ohmic drop of ~10 Ω in 1 M KOH. All the tests were carried out at room temperature (~25 °C).

Results and discussion

- Characterizations of the as-prepared samples

The successful synthesis of NiO/C nanocomposites by the procedure outlined in Fig. 1. The NiO/C nanocomposites were fabricated via a green chemical route which combined hydrothermal method and pyrolysis. The surface morphologies of carbonization of ESM, NiO particles and NiO/C nanocomposites were observed by SEM and TEM. The SEM images of the above samples can be seen in Fig. 2. As shown in Fig. 2a-b, it exhibits uniformly structure and high surface porosity with smooth surface after carbonization of ESM. And the carbonized sample seemed to easily provide more open space for anchoring nanoparticles [33]. Then NiO particles, were used simple method that combined hydrothermal approach and pyrolysis, is presented in Fig. 2c-d. It can be clearly seen that most of the particles were aggregated and with different sizes (~4 ± 1 μm). And it can be said that the structural morphology of the NiO particles is the result of two factors: the formation of $Ni(OH)_2$ happened in liquid environment without dispersed protection and the particles easily aggregated during pyrolysis. The carbonization of ESM and NiO particles were also confirmed by using EDS technique (Fig. 1S in Supporting information). However, there was a morphological difference observed from the single component, that NiO particles and carbonization of ESM, with the hybrid nanocomposites. In Fig. 2e-f, the NiO nanoparticles are homogeneously distributed on the curly surface of the carbonized nanosheet. There are two possibly reasons for this phenomenon, (1) Ni(II) ions were absorbed on the surface of ESM, then $Ni(OH)_2$ would grew on the surface of ESM uniformly after OH^- was introduced into eggshell reactor. (2) $Ni(OH)_2$/ESM was carbonized into NiO/C nanocomposites after high temperature procedures [25], therefore the carbonized ESM keep the positions of Ni(II) stable in the process, as shown in Fig. 1. Finally, the successful synthesis of NiO/C

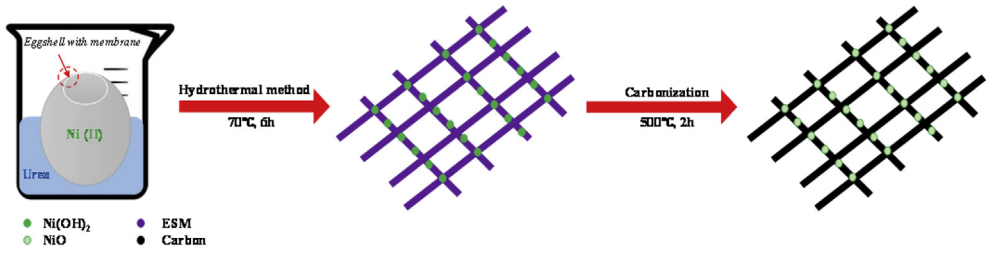

Fig. 1 – Schematic diagram for the formation of NiO/C nanocomposites.

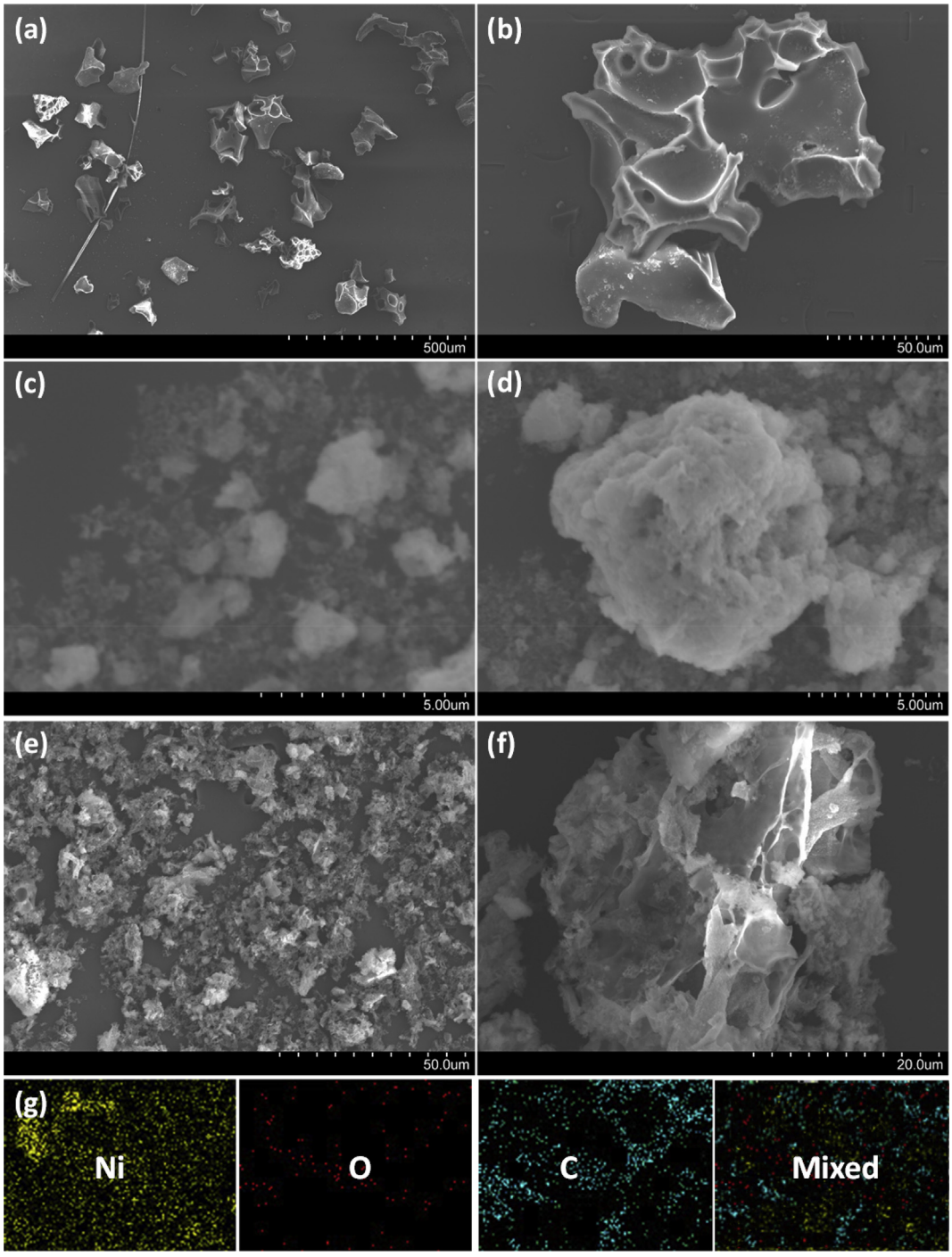

Fig. 2 – SEM images of: (a–b) carbonization of ESM, (c–d) NiO powders, (e–f) NiO/C nanocomposites. (g) EDS elemental mapping images of the NiO/C nanocomposites.

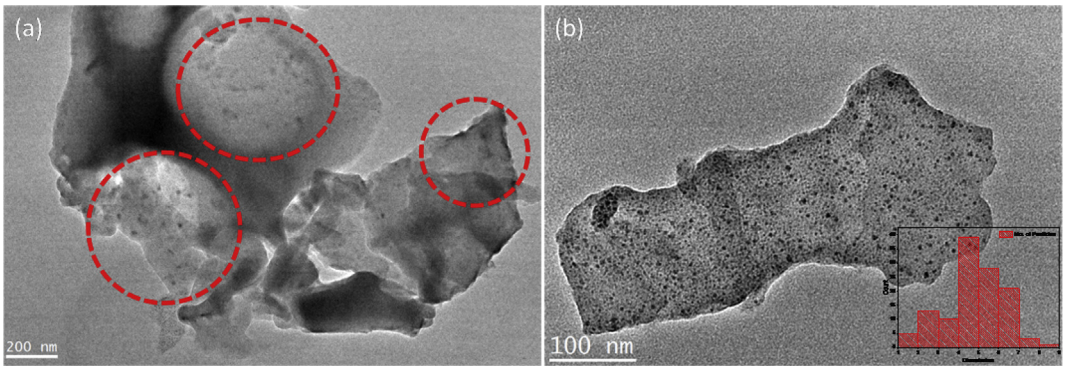

Fig. 3 – TEM images for NiO/C nanocomposites with different magnifications, (a) 200 nm and (b) 100 nm.

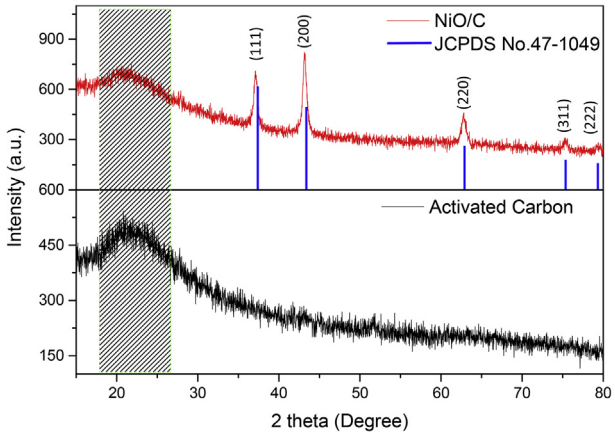

Fig. 4 – The XRD patterns of carbonization of ESM (*black* line), NiO/C (red line) and NiO's JCPDS card (blue line). (For interpretation of the references to colour in this figure legend, the reader is referred to the Web version of this article.)

nanocomposites were also confirmed by corresponding Ni, O and C elemental mapping (Fig. 2g).

The morphological structure of NiO/C nanocomposites were further investigated by TEM images. Fig. 3a-b shows the different magnification of NiO/C nanocomposites. It reveals that there are a large number of nanoparticles anchored on the surface of carbonization of ESM without any appearance of particle agglomeration. From the histogram shown insert Fig. 3b, it can be calculated that the average size of NiO in NiO/C nanocomposites is approximately 5 ± 1 nm (Fig. 2S). The NiO particles in the eggshell reactor formed at smaller diameters (5 ± 1 nm) compared to the control (4 ± 1 nm). This difference is possibly due to the protection of the eggshell membrane, avoiding the directly contact between Ni(II) ions and OH^- in solution [34]. The carbonized ESM provided more conductive media for NiO nanoparticles [28], simultaneously, the density of NiO nanoparticles increased due to shrink of ESM during carbonization [21]. This change may also bring the enhancement of catalytic performance toward the hydrogen evolution. Therefore, carbonization of ESM plays an important role in passivating the nanoparticles from further growth and provides a narrow particle size distribution of the NiO nanoparticles.

To further investigate the phase purity and crystalline structure, the as-prepared samples were examined by X-ray diffraction (XRD). As shown in Fig. 4, it displays the XRD patterns of the comparison sample (activated carbon) and the as-obtained NiO/C nanocomposites which synthesized by the two-step approach. There are five well-defined diffraction peaks at 37.2, 43.2, 62.8, 75.4 and 79.4° (2theta), which are well indexed to (111), (200), (220), (311), and (222) crystal planes indicated that the formation of NiO nanoparticles from the intermediated, $Ni(OH)_2$. The nature and positions of the above XRD result are in good agreement with standard XRD data (JCPDS No. 47-1049) and other previously reported researches [16], and NiO nanoparticles shows the cubic (fcc) phase. In addition, the diffraction angle (2theta) around 24° is amorphous carbon (JCPDS No. 41-1487). It also proved that this as-prepared activated carbon is made of amorphous carbon. No peaks from other impurities such as $Ni(OH)_2$ were observed. Furthermore, the as-obtained nanocomposites are confirmed the existence of NiO nanoparticles and amorphous carbon and without any detectable impurities. The co-existence of NiO nanoparticles and amorphous carbon peaks in XRD pattern confirms that the NiO/C nanocomposites are synthesized well. The XRD and SEM characterization results are in line with TEM observation and EDS results (Figs. 2, 4 and 1S).

Formation mechanism

From the observed SEM, EDS, TEM and XRD results, the possible pathway for the formation of the NiO/C nanocomposites was proposed. The whole process mainly undergoes the following three steps as presented in Fig. 5. At first, urea acts as the hydrolysis agent which decomposes to form OH^- ion in aqueous conditions as $Ni(NO_3)_2\,6H_2O$ solution was added into the empty eggshell, Ni^{2+} ions were gradually absorbed on the surface of ESM through the pore of ESM (blue layer). Then, the ESM served as bio-template to provide a reactor for Ni^{2+} ion and OH^- ion to form $Ni(OH)_2$. The relative reactions are presented as follows [31,35]:

$$CO(NH_2)_2 + H_2O \rightarrow CO_2\uparrow + 2NH_3\uparrow \quad (1)$$

$$NH_3 + H_2O \rightarrow NH_4^+ + OH^- \quad (2)$$

$$Ni^{2+} + 2OH^- \rightarrow Ni(OH)_2\downarrow \quad (3)$$

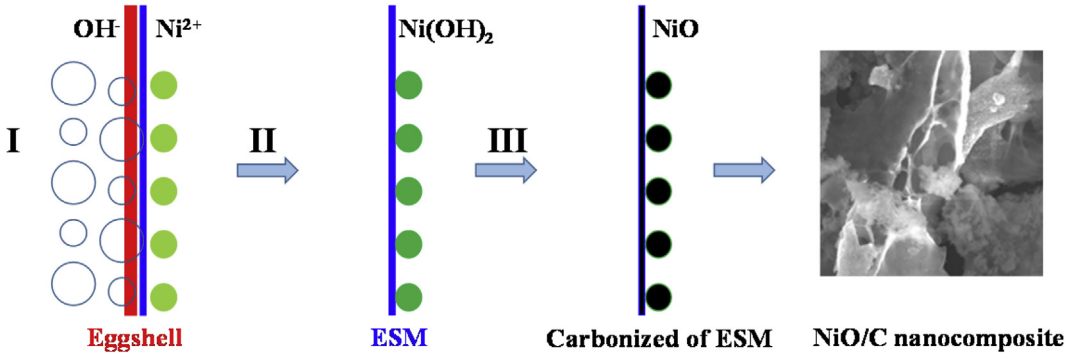

Fig. 5 – Schematic illustration of proposed formation mechanism of NiO/C nanocomposites.

After this process, the resultant $Ni(OH)_2$/ESM hybrids had a morphology very similar to the ESM template. Finally, $Ni(OH)_2$/ESM hybrids were transformed into NiO/C nanocomposites after carbonization. The $Ni(OH)_2$ formed-nanoparticles, rather than aggregated powders or particles because the ESM provides specific porous sites for Ni^{2+} ions, and prevents aggregation of $Ni(OH)_2$ during drying and carbonization. Therefore, NiO/C nanocomposites were successfully constructed via a hydrothermal and pyrolysis approach by using ESM as the carbon source.

HER performance of the NiO/C nanocomposite

The HER performance of NiO/C nanocomposites was tested by linear sweep voltammetry technique (LSV) by sweeping the potential from 0.05 V to negative potentials in 1.0 M KOH solution with a scan rate of 5 mV/s. Fig. 6a exhibits that the polarization curve for NiO/C nanocomposites modified electrode (red line), named NiO/C@GCE. For comparison, we also investigated bare GCE, carbonization of ESM modified electrode and NiO particles modified electrode, called GCE (black line), C@GCE (pink line) and NiO/GCE (blue line), respectively, as presented in Fig. 6a. The overpotential of NiO@GCE to reach at -10 mA/cm^2 and -30 mA/cm^2 were 670 mV and 753 mV respectively. Additionally, the open circuit potential (E_{oc}) of NiO@GCE is obviously lower than ideal NiO *vs.* 0.132 V_{RHE} [36]. It may due to the structure of NiO (Fig. 2c-d) and aggregation of NiO particles reducing the number of active sites, decreasing electron transfer rate during the HER process, compared with NiO nanoparticles in Fig. 2e-f. In another comparison of carbonization of ESM, C@GCE, it has better performance with values of 617 mV and 688 mV at -10 mA/cm^2 and -30 mA/cm^2 respectively, than NiO@GCE did. The overpotential of the reported current density of -10 mA/cm^2 and -30 mA/cm^2 of NiO/C@GCE is 565 mV and 644 mV, respectively. This HER activity is better than pure NiO and carbonization of ESM, indicating that NiO/C@GCE can reach higher current density than NiO@GCE and C@GCE under the same testing conditions. It is also easier found the hydrogen bubble released during NiO/C@GCE'LSV test (inset of Fig. 6a). Here, carbonization of ESM played a support for NiO nanoparticles to reduce aggregation [37,38], as can be seen from TEM images. This is due to the coupling effect of carbon with NiO nanoparticles, which greatly improves the conductivity of nanocomposites and electron transfer rate [16,39].

The HER kinetics of the catalysts were further studied by corresponding Tafel slopes. Actually, the Tafel slope derived from the polarization curves by fitting into the Tafel equation:

$$\eta = a + b^{*}\log[\text{-current density}]$$

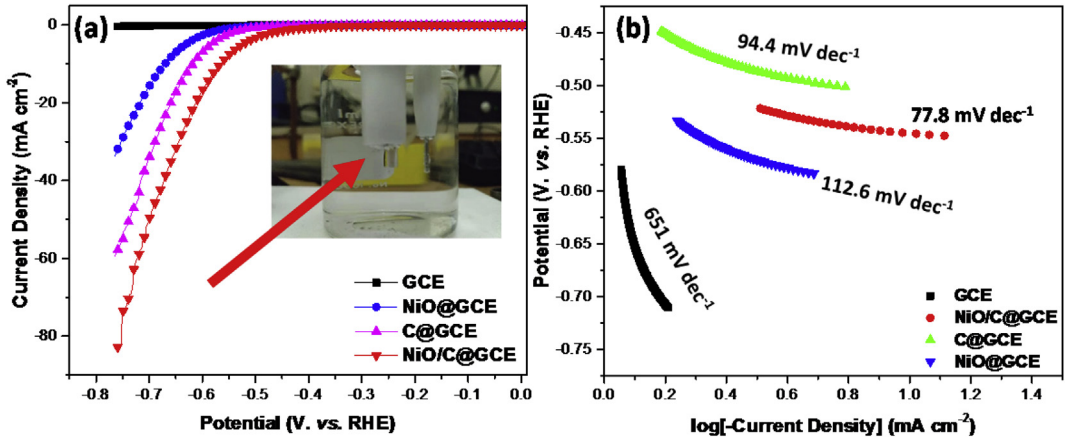

Fig. 6 – (a) Comparison of the polarization curves of GCE, NiO@GCE, C@GCE and NiO/C@GCE, scan rate: 5 mV/s, inset: image of HER process; (b) Tafel plots of GCE, NiO@GCE, C@GCE and NiO/C@GCE in an N_2-saturated 1M KOH solution.

Table 1 – Comparison of Tafel slope value of various electrocatalysts.

Catalyst	Tafel slope/mV dec^{-1}	Overpotential/mV@10 mA cm^{-2}	Medium	Reference
C@NiO/Ni nanofibers	152	~425	Alkaline	[16]
Ni/NiO	244	N/A	Alkaline	[9]
$CoNi_2S_4$	85	255	Alkaline	[41]
$NiCo_2O_4$/CuS carbon fiber paper	41	72.3	Acidic	[42]
Ni/NiO/C	44	102	Acidic	[43]
NiO/C nanocomposites	77.8	565	Alkaline	this work

where, b is the Tafel slope, as presented in Fig. 6b.

The NiO/C@GCE shows smaller Tafel slope (77.8 mV dec^{-1}) as compared to NiO@GCE's Tafel slope (112.6 mV dec^{-1}) and C@GCE's Tafel slope (94.4 mV dec^{-1}) respectively. This result also supported the enhanced HER activity of NiO/C@GCE via coupling effect between the HER performances of NiO@GCE and C@GCE. Normally, HER process often includes three typical reactions (I) Volmer reaction, (II) Heyrovsky reaction and (III) Tafel reaction, corresponding the different Tafel slopes of 120, 40 and 30 mV dec^{-1}, respectively, as shown in Equations (4)–(6). However, there are two possible pathways in alkaline solution: they have same start procedure producing H adsorbed (H_{ads}), which H_2O molecule was adsorbed on the surface of electrode via molecule interaction and electrochemical reduction (Equation 4). Then for the (1) pathway, the next step is H_2O molecule is reacted with H_{ads} in order to obtain H_2 (Equation 5). But for the (2) pathway, the continued step is that different H_{ads} reacted each other generating H_2 directly (Equation 6). Consequently, the experimentally measured Tafel slope of 77.8 mV dec^{-1} for NiO/C@GCE indicates that the HER occurred by Volmer-Heyrovsky mechanism [18,40]. The comparison list of Tafel slope of the various electrocatalysts is reported in Table 1. NiO/C nanocomposites showed higher Tafel slope value as compared with the other metal oxides-based catalyst reported in the literatures.

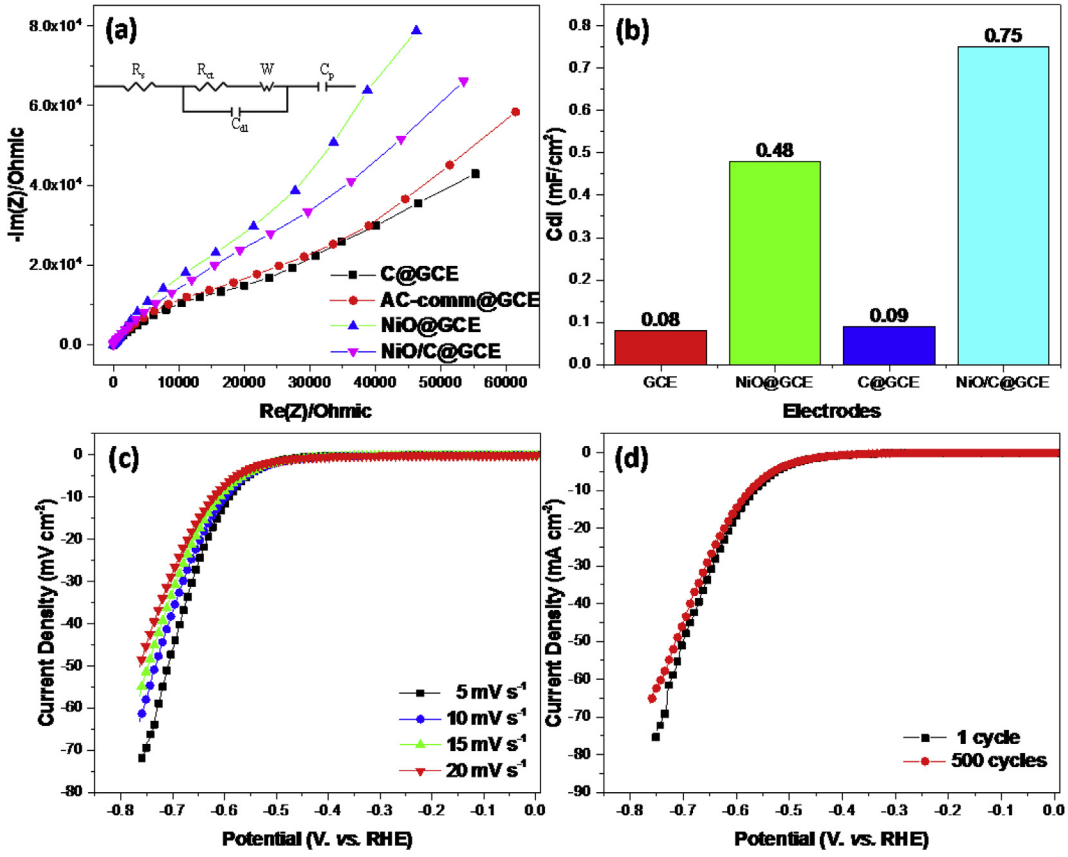

Fig. 7 – (a) EIS plots of C@GCE, AC-comm@GCE, NiO@GCE and NiO/C@GCE at 0.10 V vs. RHE, Inset: equivalent circuit; (b) Current density differences plotted as a function of the potential scan rate (the slope for C_{dl}) pink plots for GCE, black for NiO/GCE, blue for C@GCE and red for NiO/C@GCE; (c) Polarization curves of NiO/C nanocomposites at different scan rates. (d) Durability testing of NiO/C@GCE by cycling the electrode between 0.25 and 0.55 V in an N_2-saturated 1M KOH solution. (For interpretation of the references to colour in this figure legend, the reader is referred to the Web version of this article.)

$$H_2O + e^- \rightarrow H_{ads} + OH^- \text{ Volmer} \quad (4)$$

$$H_2O + H_{ads} \rightarrow H_2 + OH^- \text{ Heyrovsky} \quad (5)$$

$$H_{ads} + H_{ads} \rightarrow H_2 \text{ Tafel} \quad (6)$$

To probe the reasons for the enhanced electrocatalytic performances of the NiO/C nanocomposites, the electrochemical impedance spectroscopy (EIS), the CV and LSV techniques were also employed. The EIS test was employed to evaluate the transport kinetics for electrochemical reaction process. Fig. 7a shows that the Nyquist plots of NiO/C and activated carbon (Commercial product, as comparison), it is obviously observed that the Nyquist plot of NiO/C is almost linear, while that of the carbonization of ESM and activated carbon with similar trend which consists of a quasi-semicircular arch at high frequencies and an oblique line at low frequencies. It is well established that a larger semicircle means a larger charge transfer resistance (R_{ct}) and a steeper slope represents a lower resistance of electrolyte ions (Warburg impendence, Z_w). According to the Nyquist plot fitted by the equivalent circuit (inset of Fig. 7a), the R_{ct} of NiO/C nanocomposites, carbonization of ESM, activated carbon and NiO particles are 0.68, 1.04, 0.97 and 1.06 Ω, respectively. Thus, it is obvious that the NiO/C composite has a smaller R_{ct} than the carbonization of ESM and NiO particles. This indicates that the as-prepared nanocomposites has a faster electron transfer process due to the coupling effect between carbonization of ESM and NiO nanoparticles. In additional, the double-layer capacitances (C_{dl}) which is linearly proportional to the effective electrochemical active surface area, were also calculated (Fig. 3S). We found that the C_{dl} of NiO/C was significantly higher 1.5 times than NiO's, though the C_{dl} of NiO is only 0.48 mF cm^{-2} (Fig. 7b). We believe that this larger effective active surface area is due to more uniform distribution of NiO nanoparticles on the surface of carbonization of ESM, as can be found from the TEM images. Besides, we found the carbonization of ESM and activated carbon has similar electrochemical properties in terms of R_{ct} and C_{dl}, it also confirmed the performance of carbonization of ESM can replace commercial activated carbon. Overall, the smaller R_{ct} and the larger C_{dl} suggest achievement of synergistically electronic and structural modulations for HER performance between the carbonization of ESM and the NiO nanoparticles.

The influence of scan rate was also tested by conducting LSV curves with a NiO/C@GCE. According to the LSV curves (Fig. 7c), the current density increases at the same potential with increasing scan rate. Because larger scan rate induces larger reaction current and electric double layer charging current [44]. As a result, more hydrogen were generated and easily diffused from the surface of the working electrode. All these factors should contribute to the enhanced catalytic performance of the NiO/C nanocomposites. Finally, the stability of the NiO/C nanocomposite was also evaluated by conducting CV test between 0.25 V and 0.55 V in 1 M KOH solution. As can be seen from Fig. 7d, after 500 cycles, change of the current density at certain overpotential is small. Although metal oxides are not shown good performance on HER, the as-prepared NiO/C nanocomposites showed a good durability [4,10].

Conclusion

In summary, NiO/C nanocomposite derived from $Ni(OH)_2$/ESM composite was successfully prepared by a facile and green approach that combined simple hydrothermal and pyrolysis method. Here, the waste eggshell was regard as an useful resource for the as-synthesized sample, it not only provides ESM for the adsorbed Ni(II) ions, but only works as a reactor for this preparation. Consequently, it has been observed that NiO nanoparticles distributed on the surface of ESM uniformly. The as-prepared NiO/C nanocomposite showed stable electrocatalytic and high activity towards HER in alkaline solution, it also needs lower overpotential of 565 mV to drive −10 mA cm^{-2} with Tafel slope of 77.8 mV dec^{-1} than the compared samples. Moreover, the preparation approach addressed a facile, economic and green strategy for the preparation of other metal oxides with carbon support and provided an important example for the strategy to enhance their electrical conductivity and improve their HER performance in alkaline solution.

Acknowledgement

This work was supported by NASA EpsCor (No. NNX16AQ98A), USDA-NIFA Sungrant (North Central: 2014-38502-22598), USDA-NIFA (No. 11903497) and USDA-NIFA Hatch (No. SD00H618-16) for research support, and S. Lu thanks K. Chen and S. G. Wang for their care in my first three months in U.S.

Appendix A. Supplementary data

Supplementary data to this article can be found online at https://doi.org/10.1016/j.ijhydene.2019.04.191.

REFERENCES

[1] Zhao GQ, Rui K, Dou SX, Sun WP. Heterostructures for electrochemical hydrogen evolution reaction: a review. Adv Funct Mater 2018;28:1803291.
[2] Sinigaglia T, Lewiski F, Martins MES, Siluk JCM, et al. Production, storage, fuel stations of hydrogen and its utilization in automotive applications-a review. Int J Hydrogen Energy 2017;42:24597–611.
[3] Zhou W, Jia J, Lu J, Yang L, Hou D, Li G, et al. Recent developments of carbon-based electrocatalysts for hydrogen evolution reaction. Nano Energy 2016;28:29–43.
[4] Zhang T, Wu MY, Yan DY, Mao J, Liu H, Hu WB, et al. Engineering oxygen vacancy on NiO nanorod arrays for alkaline hydrogen evolution. Nano Energy 2018;43:103–9.
[5] Safizadeh F, Ghali E, Houlachi G, et al. Electrocatalysis developments for hydrogen evolution reaction in alkaline solutions-a review. Int J Hydrogen Energy 2015;40:256–74.
[6] Zou X, Zhang Y. Noble metal-free hydrogen evolution catalysts for water splitting. Chem Soc Rev 2015;44:5148–80.

[7] Yin H, Zhao S, Zhao K, Muqsit A, Tang H, Chang L, et al. Ultrathin platinum nanowires grown on single-layered nickel hydroxide with high hydrogen evolution activity. Nat Commun 2015;6:6430.
[8] Cheng N, Stambula S, Wang D, Banis MN, Liu J, Riese A, et al. Platinum single-atom and cluster catalysis of the hydrogen evolution reaction. Nat Commun 2016;7:13638.
[9] Chen ZH, Ma ZP, Song JJ, Wang LX, Shao GJ. Novel one-step synthesis of wool-ball-like Ni-carbon nanotubes composite cathodes with favorable electrocatalytic activity for hydrogen evolution reaction in alkaline solution. J Power Sources 2016;324:86–96.
[10] Zheng Y, Jiao Y, Vasileff A, Qiao SZ. The hydrogen evolution reaction in alkaline solution: from theory, single crystal models, to practical electrocatalysts. Angew Chem Int Ed 2018;57:7568–79.
[11] Gong M, Zhou W, Tsai MC, Zhou J, Guan M, Lin MC, et al. Nanoscale nickel oxide/nickel heterostructures for active hydrogen evolution electrocatalysis. Nat Commun 2014;5:4695.
[12] Liu T, Jiang CJ, Cheng B, You W, Yu JG. Hierarchical flower-like C/NiO composite hollow microspheres and its excellent supercapacitor performance. J Power Sources 2017;359:371–8.
[13] Li T, Li XH, Wang ZX, Guo HJ, Li Y, Wang JX. A new design concept for preparing nickel-foam supported metal oxide microspheres with superior electrochemical properties. J Mater Chem A 2017;5:13469–74.
[14] Czelej K, Cwieka K, Colmenares JC, Kurzydlowski KJ. Catalytic activity of NiO cathode in molten carbonate fuel cells. Appl Catal B Environ 2018;222:73–5.
[15] Li YH, Liu PF, Pan LF, Wang HF, Yang ZZ, Zheng LR, et al. Local atomic structure modulations activate metal oxide as electrocatalyst for hydrogen evolution in acidic water. Nat Commun 2015;6:8064.
[16] Chinnappan A, Ji DX, Jayathilaka WADM, Baskar C, Qin XH, Ramakrishna S. Facile synthesis of electrospun C@NiO/Ni nanofibers as an electrocatalyst for hydrogen evolution reaction. Int J Hydrogen Energy 2018;43:15217–24.
[17] Yang Y, Yang F, Hu HR, Lee SS, Wang Y, Zhao HR, et al. Dilute NiO/carbon nanofiber composites derived from metal organic framework fibers as electrode materials for supercapacitors. Chem Eng J 2017;307:583–92.
[18] Xu YF, Gao MR, Zheng YR, Jiang J, Yu SH. Nickel/nickel(II) oxide nanoparticles anchored onto cobalt(IV) diselenide nanobelts for the electrochemical production of hydrogen. Angew Chem Int Ed 2013;52:8546–50.
[19] Meng XH, Deng D. Trash to treasure: waste eggshells used as reactor and template for synthesis of Co_9S_8 nanorod arrays on carbon fibers for energy storage. Chem Mater 2016;28:3897–904.
[20] Tembe S, Kubal BS, Karve M, D'Souza SF. Glutaraldehyde activated eggshell membrane for immobilization of tyrosinase from amorphophallus companulatus: application in construction of electrochemical biosensor for dopamine. Anal Chim Acta 2008;612:212–7.
[21] Deng WT, Liu Y, Zhang Y, Lu F, Chen QY, Ji XB. Enhanced electrochemical capacitance of nanoporous NiO based on an eggshell membrane. RSC Adv 2012;2:1743–5.
[22] Nguyen VH, Lee DH, Baek SY, Kim YH. Recycling different eggshell membranes for lithium-ion battery. Mater Lett 2018;228:504–8.
[23] Ma LB, Chen RP, Hu Y, Zhang WJ, Zhu GY, Zhao PY, et al. Nanoporous and lyophilic battery separator from regenerated eggshell membrane with effective suppression of dendritic lithium growth. Energy Storage Mater 2018;14:258–66.
[24] Park S, Choi KS, Lee D, Kim D, Lim KT, Lee KH, et al. Eggshell membrane: review and impact on engineering. Biosyst Eng 2016;151:446–63.
[25] Meng XH, Deng D. Bio-inspired synthesis of 3-D network of NiO-Ni nanowires on carbonized eggshell membrane for lithium-ion batteries. Chem Eng Sci 2019;194:134–41.
[26] Huang L, Li J, Wang Z, Li Y, He X, Yuan Y. Microwave absorption enhancement of porous C@$CoFe_2O_4$ nanocomposites derived from eggshell membrane. Carbon 2019;143:507–16.
[27] Selvakumari JC, Nishanthi ST, Dhanalakshmi J, Ahila M, Padiyan DP. Bio-active synthesis of tin oxide nanoparticles using eggshell membrane for energy storage application. Appl Surf Sci 2018;441:530–7.
[28] Chung SH, Manthiram A. Carbonized eggshell membrane as a natural polysulfide reservoir for highly reversible Li-S batteries. Adv Mater 2014;26:1360–5.
[29] Yu H, Tang Q, Wu J, Lin Y, Fan L, Huang M, et al. Using eggshell membrane as a separator in supercapacitor. J Power Sources 2012;206:463–8.
[30] Zhang ZC, Xu B, Wang X. Engineering nanointerfaces for nanocatalysis. Chem Soc Rev 2014;43:7870–86.
[31] Lu S, Yang C, Nie M. Hydrothermal synthesized urchin-like nickel-cobalt carbonate hollow spheres for sensitive amperometric detection of nitrite. J Alloy Compd 2017;708:780–6.
[32] Meng XH, Deng D. Trash to treasure: waste eggshells as chemical reactors for the synthesis of amorphous $Co(OH)_2$ nanorod arrays on various substrates for applications in rechargeable alkaline batteries and electrocatalysis. ACS Appl Mater Interfaces 2017;9:5244–53.
[33] Hou HS, Jing MJ, Yang YC, Zhang Y, Song WX, Yang XM, et al. Antimony nanoparticles anchored on interconnected carbon nanofibers networks as advanced anode material for sodium-ion batteries. J Power Sources 2015;284:227–35.
[34] Li Y, Xie X, Liu J, Cai M, Rogers J, Shen W. Synthesis of α-$Ni(OH)_2$ with hydrotalcite-like structure: precursor for the formation of NiO and Ni nanomaterials with fibrous shapes. Chem Eng J 2008;136:398–408.
[35] Tian JY, Shao Q, Dong XJ, Zheng JL, Pan D, Zhang XY, et al. Bio-template synthesized NiO/C hollow microspheres with enhanced Li-ion battery electrochemical performance. Electrochim Acta 2018;261:236–45.
[36] Hall DS, Bock C, MacDougall BR. The electrochemistry of metallic nickel: oxides, hydroxides, hydrides and alkaline hydrogen evolution. J Electrochem Soc 2013;160:F235–43.
[37] Zhang LL, Zhu SQ, Dong SY, Woo NJ, Xu ZL, Huang JQ, et al. Co nanoparticles encapsulated in porous N-doped carbon nanofibers as an efficient electrocatalyst for hydrogen evolution reaction. J Electrochem Soc 2018;165:J3271–5.
[38] Wang DY, Gong M, Chou HL, Pan CJ, Chen HA, Wu Y, et al. Highly active and stable hybrid catalyst of cobalt-doped FeS^2 nanosheets-carbon nanotubes for hydrogen evolution reaction. J Am Chem Soc 2015;137:1587–92.
[39] Ji DX, Peng SJ, Lu J, Li LL, Yang SY, Yang GR, et al. Design and synthesis of porous channel-rich carbon nanofibers for self-standing oxygen reduction reaction and hydrogen evolution reaction bifunctional catalysts in alkaline medium. J Mater Chem A 2017;5:7507–15.
[40] Liu YY, Zhang HP, Zhu B, Zhang HW, Fan LD, Chai XY, et al. C/N-co-doped Pd coated Ag nanowires as a high-performance electrocatalyst for hydrogen evolution reaction. Electrochim Acta 2018;283:221–7.
[41] Wang DZ, Zhang XY, Du ZJ, Mo ZY, Wu YF, Yang Q, et al. $CoNi_2S_4$ nanoparticles as highly efficient electrocatalysts for

the hydrogen evolution reaction in alkaline media. Int J Hydrogen Energy 2017;42:3043–50.
[42] An L, Huang L, Zhou PP, Yin J, Liu HY, Xi PX. A self-standing high-performance hydrogen evolution electrode with nanostructured $NiCo_2O_4$/CuS heterostructures. Adv Funct Mater 2015;25:6814–22.
[43] Chu M, Wang L, Li X, Hou MJ, Li N, Dong YZ, et al. Carbon coated nickel-nickel oxide composites as a highly efficient catalyst for hydrogen evolution reaction in acid medium. Electrochim Acta 2018;264:284–91.
[44] Jin J, Zhu Y, Liu Y, Li Y, Peng W, Zhang G, et al. CoP nanoparticles combined with WS_2 nanosheets as efficient electrocatalytic hydrogen evolution reaction catalyst. Int J Hydrogen Energy 2017;42:3947–54.